HHS Public Access

Author manuscript

Genes Chromosomes Cancer. Author manuscript; available in PMC 2014 June 11.

Published in final edited form as:

Genes Chromosomes Cancer. 2014 February ; 53(2): 183–193. doi:10.1002/gcc.22132.

Novel *ZC3H7B-BCOR, MEAF6-PHF1* and *EPC1-PHF1* Fusions in Ossifying Fibromyxoid Tumors – Molecular Characterization Shows Genetic Overlap with Endometrial Stromal Sarcoma

Cristina R Antonescu[1], **Yun-Shao Sung**[1], **Chun-Liang Chen**[1], **Lei Zhang**[1], **Hsiao-Wei Chen**[1], **Samuel Singer**[2], **Narasimhan P Agaram**[1], **Andrea Sboner**[3,4,5], and **Christopher D Fletcher**[6]

[1]Department of Pathology, Memorial Sloan-Kettering Cancer Center, New York, NY

[2]Department of Surgery, Memorial Sloan-Kettering Cancer Center, New York, NY

[3]Department of Pathology and Laboratory Medicine, Weill Cornell Medical College, New York, NY

[4]Institute for Computational Biomedicine, Weill Medical College of Cornell University, New York, NY

[5]Institute for Precision Medicine, Weill Medical College of Cornell University and New York Presbyterian Hospital, New York, NY

[6]Department of Pathology, Brigham and Women's Hospital, Boston, MA

Abstract

PHF1 gene rearrangements have been recently described in around 50% of ossifying fibromyxoid tumors (OFMT) including benign and malignant cases, with a small subset showing *EP400-PHF1* fusions. In the remaining cases no alternative gene fusions have been identified. *PHF1*-negative OFTs, especially if lacking S100 protein staining or peripheral ossification, are difficult to diagnose and distinguish from other soft tissue mimics. In seeking more comprehensive molecular characterization, we investigated a large cohort of 39 OFMT of various anatomic sites, immunoprofiles and grades of malignancy. Tumors were screened for *PHF1* and *EP400* rearrangements by FISH. RNA sequencing was performed in two index cases (OFMT1, OFMT3), negative for *EP400-PHF1* fusions, followed by FusionSeq data analysis, a modular computational tool developed to discover gene fusions from paired-end RNA-seq data. Two novel fusions were identified *ZC3H7B-BCOR* in OFMT1 and *MEAF6-PHF1* in OFMT3. After being validated by FISH and RT-PCR, these abnormalities were screened on the remaining cases. With these additional gene fusions, 33/39 (85%) of OFMTs demonstrated recurrent gene rearrangements, which can be used as molecular markers in challenging cases. The most common abnormality is *PHF1* gene rearrangement (80%), being present in benign, atypical and malignant lesions, with fusion to *EP400* in 44% of cases. *ZC3H7B-BCOR* and *MEAF6-PHF1* fusions occurred predominantly in S100 protein-negative and malignant OFMT. As similar gene fusions were

Correspondence: Cristina R Antonescu, Memorial Sloan-Kettering Cancer Center, 1275 York Ave, New York, NY 10021, antonesc@mskcc.org; and Christopher Fletcher, Brigham and Women's Hospital, 75 Francis Street, Boston, MA 02115, cfletcher@partners.org.

Conflict of interest: none

reported in endometrial stromal sarcomas, we screened for potential gene abnormalities in *JAZF1* and *EPC1* by FISH and found two additional cases with *EPC1-PHF1* fusions.

Keywords

Ossifying fibromyxoid tumor; PHF1; EP400; BCOR; MEAF6

INTRODUCTION

OFMT is a rare soft tissue tumor of uncertain lineage, characterized histologically by multinodular growth and a distinctive shell of mature bone found at the periphery of the nodules. Microscopically, the tumors are composed of uniform round to oval cells embedded in a fibro-myxoid stroma. The tumors are often positive for S100 protein; however, the significance of this finding remains puzzling, since electron microscopic studies have failed to pinpoint a line of differentiation, excluding schwannian, melanocytic, chondroid or myoepithelial differentiation. In addition to its controversial histogenesis, the criteria for malignancy are not well defined, and atypical/malignant forms often deviate from the classic morphology, with lack of S100 protein expression or peripheral ossification. In the absence of objective molecular markers these atypical examples are difficult to distinguish from other look-alike soft tissue lesions.

The *PHF1* gene, previously shown to be the 3′-partner of fusion genes in endometrial stromal tumors, has recently been implicated in the pathogenesis of about 50% of OFMTs, irrespective of whether they are diagnosed as typical, atypical, or malignant lesions (Gebre-Medhin et al., 2012; Graham et al., 2013). In only two tumors *PHF1* was shown to fuse to *EP400* (Gebre-Medhin et al., 2012; Endo et al., 2013), while in the remaining cases no alternative gene partners have been identified as yet. In this study we performed a detailed molecular analysis in a large cohort of OFMT lesions, covering a wide spectrum of clinical presentations and degree of malignancy. *EP400-PHF1* negative tumors were investigated by RNA sequencing for novel translocation discovery and validated abnormalities were then screened in the remaining cases.

MATERIAL AND METHODS

The Pathology files of MSKCC and the personal consultations of the corresponding authors (CRA, CDF) were searched for cases of ossifying fibromyxoid tumor (OFMT), of any degree of malignancy. Pathologic diagnosis and immunohistochemical stains were re-reviewed in all cases. The histologic requirement for inclusion in the study was a predominantly classic morphologic appearance, the tumors being composed of relatively monotonous epithelioid, cuboidal or oval cells, arranged in cords or single files within a fibromyxoid stroma. Cases that displayed significant nuclear pleomorphism or conspicuous areas of spindling and fascicular growth were excluded. OFMT were classified as benign, for tumors with typical morphologic features and lacking cytologic atypia or increased mitotic activity. Tumors with increased cellularity but lacking increased mitotic activity, necrosis or nuclear pleomorphism were defined as atypical OFMTs. Malignant OFMTs showed increased cellularity, mitotic activity (>2MF/50HPFs) and/or nuclear pleomorphism

or necrosis. The presence of ossification defined as a rim of lamellar bone was recorded in every case. Additional osteoid-like matrix deposition, if present, was separately recorded. Immunohistochemical stains, including S100 protein and desmin, were reviewed and results were correlated with degree of malignancy and fusion type (Table 1). The study was approved by the Institutional Review Board 02-060.

RNA Sequencing

Total RNA was prepared for RNA sequencing in accordance with the standard Illumina mRNA sample preparation protocol (Illumina). Briefly, mRNA was isolated with oligo(dT) magnetic beads from total RNA (10 μg) extracted from case. The mRNA was fragmented by incubation at 94°C for 2.5 min in fragmentation buffer (Illumina). To reduce the inclusion of artifactual chimeric transcripts due to random priming of transcript fragments into the sequencing library because of inefficient A-tailing reactions that lead to self ligation of blunt-ended template molecules (Quail et al., 2008), an additional size-selection step (capturing 350–400 bp) was introduced prior to the adapter ligation step. The adaptor-ligated library was then enriched by PCR for 15 cycles and purified. The library was sized and quantified using DNA1000 kit (Agilent) on an Agilent 2100 Bioanalyzer according to the manufacturer's instructions. Paired-end RNA-sequencing at read lengths of 50 or 51 bp was performed with the HiSeq 2500 (Illumina). Across the two samples a total of about 141 million paired-end reads were generated, corresponding to about 21 billion bases.

Analysis of RNA Sequencing Results with FusionSeq

All reads were independently aligned with STAR alignment software against the human genome reference sequence (hg19) and a splice junction library, simultaneously (Dobin et al., 2013). The mapped reads were converted into Mapped Read Format (Habegger et al., 2011) and analyzed with FusionSeq (Sboner et al., 2010) to identify potential fusion transcripts. FusionSeq is a computational method successfully applied to paired-end RNA-seq experiments for the identification of chimeric transcripts (Tanas et al., 2011; Pierron et al., 2012) (Mosquera et al., 2013). Briefly, paired-end reads mapped to different genes are first used to identify potential chimeric candidates. A cascade of filters, each taking into account different sources of noise in RNA-sequencing experiments, was then applied to remove spurious fusion transcript candidates. Once a confident list of fusion candidates was generated, they were ranked with several statistics to prioritize the experimental validation. In these cases, we used the DASPER score (Difference between the observed and Analytically calculated expected SPER): a higher DASPER score indicated a greater likelihood that the fusion candidate was authentic and did not occur randomly. See (Sboner et al., 2010) for further details about FusionSeq.

Fluorescence In Situ Hybridization (FISH)

FISH on interphase nuclei from paraffin-embedded 4-micron sections was performed applying custom probes using bacterial artificial chromosomes (BAC), covering and flanking genes that were identified as potential fusion partners in the RNA-seq experiment. BAC clones were chosen according to USCS genome browser (http://genome.uscs.edu), see Supplementary Table 1. The BAC clones were obtained from BACPAC sources of Children's Hospital of Oakland Research Institute (CHORI) (Oakland, CA) (http://

bacpac.chori.org). DNA from individual BACs was isolated according to the manufacturer's instructions, labeled with different fluorochromes in a nick translation reaction, denatured, and hybridized to pretreated slides. Slides were then incubated, washed, and mounted with DAPI in an antifade solution, as previously described (Antonescu et al., 2010). The genomic location of each BAC set was verified by hybridizing them to normal metaphase chromosomes. Two hundred successive nuclei were examined using a Zeiss fluorescence microscope (Zeiss Axioplan, Oberkochen, Germany), controlled by Isis 5 software (Metasystems). A positive score was interpreted when at least 20% of the nuclei showed a break-apart signal. Nuclei with incomplete set of signals were omitted from the score.

Reverse Transcription Polymerase Chain Reaction (RT-PCR)

An aliquot of the RNA extracted above from frozen tissue (Trizol Reagent; Invitrogen; Grand Island, NY) was used to confirm the novel fusion transcript identified by FusionSeq. RNA quality was determined by Eukaryote Total RNA Nano Assay and cDNA quality was tested for PGK housekeeping gene (247 bp amplified product). Three microgram of total RNA was used for cDNA synthesis by SuperScript ® III First-Strand Synthesis Kit (Invitrogen, Carlsbad, CA). RT-PCR was performed using the Advantage-2 PCR kit (Clontech, Mountain View, CA) for 33 cycles at a 64.5°C annealing temperature, using the following primers: ZC3H7B-Ex10F: 5′ – CCTTCGGCTTGGTCATGGAC – 3′; BCOR-Ex7R: 5′ –GAGACTTTGCGTTTCCTGTCCAC– 3′; MEAF6-Ex4F: 5′ – CAGGAGTTCAGGACCAGCTC – 3′; PHF1-Ex3R: 5′ – CCTCAAACTGGACCAGACACAC – 3′. Amplified products were purified and sequenced by Sanger method.

Long-Range PCR

Genomic DNA was extracted from frozen tissue using the Phenol/Chloroform assay and quality was confirmed by electrophoresis. 0.5 μg genomic DNA was amplified with the LongRange PCR Kit (QIAGEN, Germantown, MD) in order to assess the intronic breaks. The following primer sets were used to investigate both derivatives for each gene fusion: derivative 22: ZC3H7B-Ex10F: 5′ – CCTTCGGCTTGGTCATGGAC – 3′; BCOR-Ex7R: 5′ –GAGACTTTGCGTTTCCTGTCCAC– 3′; derivative x: BCOR-Ex6F: 5′ – CGACTGGGAAAGGTTGAAAGG – 3′; ZC3H7B-Ex12R: 5′ – GATGAGCAAGGCAGTGTTGGG – 3′; derivative 1: MEAF6-Ex5F: 5′ – CTCAGGGAGTCACCACAGCAG – 3′ ; PHF1-Ex2R: 5′ - CCAAAGTGAGGAGGCACCAG – 3′; derivative 6: PHF1-Ex1F: 5′ – CTTTGGCTGCTGCGTCATAC – 3′; MEAF6-In6R: 5′ – GGTCTCAAAAAGGCATACTGGTG – 3′.

RESULTS

Pathologic Features

Fifty OFMTs were selected for the study based on their typical morphologic appearance; however, eleven cases were subsequently excluded due to FISH failure secondary to prior decalcification. Thus the study group was composed of thirty-nine tumors, showing classic histologic features and adequate tissue for FISH. There were 22 females and 17 males, with

a mean age at diagnosis of 54 years-old (range 21–76). The tumor location included: lower extremities, 17 (thigh, 8; foot, 6; buttock/hip, 3); upper extremity, 7 (shoulder, 4; forearm, hand/finger); trunk, 9 (back/paraspinal, 3; axilla, 3; breast, 2; chest wall, 1) and head & neck, 6. Most tumors showed a multinodular growth pattern, surrounded by an incomplete fibrous pseudocapsule, which was variably ossified or hyalinized (Figs. 1A, B, D, E). Despite this rather well-defined appearance at low power, small microscopic foci were commonly present outside the fibrous capsule. Additionally, two of the superficial cases involving skin showed a diffuse, infiltrative growth up to the epidermis. In some tumors thick collagenous bands separated the tumor into large compartments (Fig. 1G).

Twenty-one cases were classified as benign, three were atypical and fifteen were malignant (Tables 1 and 2). Benign OFMT showed uniform cytomorphology, ranging from delicate, small cells with scant cytoplasm, ill-defined cell borders and uniform ovoid nuclei with fine chromatin (Fig. 1H), to more epithelioid cells with better defined cell borders and moderate amount of cytoplasm, ranging from amphophilic (Fig. 1I) to more densely eosinophilic, reminiscent of rhabdoid phenotype in two cases (Fig. 1J). Eight of the benign OFMTs showed peripheral ossification, while the remaining 13 did not. Atypical OFMT showed increased cellularity and a loose myxoid stroma, but was not accompanied by increased mitotic activity. All 3 atypical OFMTs showed areas of ossification.

Despite their increased cellularity and brisk mitotic activity (Figs. 1K–O), most malignant OFMTs did not show highly pleomorphic components or large areas of spindling/fascicular growth. Instead, the tumors had a more compact/solid architecture, composed of packed oval to short fusiform cells separated by a loose intervening myxoid stroma (Fig. 1M). The myxoid quality of the extracellular matrix predominated in the malignant examples compared to the more densely fibrous or fibromyxoid stroma in the benign cases, where tumors showed a more rigid, cord-like epithelioid morphology. Most malignant OFMTs showed a peripheral shell of lamellar bone (Figs 1A,D); except for two cases were no ossification was noted. A subset of malignant OFMT had**,** in addition to the lamellar bone areas, focal osteoid-like matrix deposition, surrounding individual tumor cells, reminiscent of an extraskeletal osteosarcoma (Fig. 1F). Only two tumors showed large areas of necrosis.

Within the entire cohort, immunohistochemical stains for S100 protein was positive in 60% and desmin in 70% of cases. Most malignant OFMTs were negative for S100 protein, with only 4 cases showing focal (Fig. 1P) or more diffuse staining. The reverse was true in the benign and atypical OFMT, most showing reactivity for S100 protein, with only 4 tumors being negative. Desmin positivity was seen in half of the malignant OFMT, but in most (71%) of benign and atypical lesions.

FusionSeq Identifies Novel Fusion Involving *ZC3H7B-BCOR*

FusionSeq identified a *ZC3H7B-BCOR* fusion as the top candidate in OFMT1, a malignant OFMT (Figs. 2A,B). Alignment of the reads suggested a fusion of *ZC3H7B* exon 10 with exon 7 of *BCOR*, fusion transcript sequence, which was then confirmed by RT-PCR (Fig. 2C). Furthermore, FISH analysis using a fusion-assay showed rearrangements in both *ZC3H7B* and *BCOR* genes (Fig. 4). Long range DNA PCR, showed the fusion of intron 10 (732bp) of *ZC3H7B* with 1306 bp of intron 6 of *BCOR* (Fig. 2D). Remaining *PHF1*-

negative cases were tested for BCOR gene abnormalities by FISH and one additional case was identified, OFMT2 (Table 1); however this lacked a break-apart signal in *ZC3H7B*. Interestingly, both cases were classified as malignant but with typical ossification, occurred in the thigh of males aged 55 and 76 respectively, and were negative for both S100 protein and desmin (Figs. 1A–C, N).

Novel *MEAF6-PHF1* Fusions in a subset of S100 protein negative OFMTs

FusionSeq identified in the 2nd index case, OFMT3, a *MEAF6-PHF1* as the top candidate. Alignment of the reads suggested a fusion of *MEAF6* exon 5 with exon 2 of *PHF1*, which was confirmed by RT-PCR (Fig. 3). Exon 1 of *PHF1* and the first 16 bp of exon 2 are untranslated. FISH confirmed the presence of *PHF1* gene rearrangement, while showed only one copy of the *MEAF6*, in keeping with an unbalanced translocation. Long Range DNA PCR also failed to identify the intronic breakpoint, using a variety of different primer strategies. The remaining *PHF1*-rearranged cases, lacking an *EP400* abnormality, were screened by FISH for potential *MEAF6* break-apart signals. Two additional cases were positive for a *MEAF6-PHF1* fusion (Fig 4, Table 1). The three *MEAF6-PHF1*-positive tumors showed a peripheral rim of lamellar bone but lacked S100 protein reactivity. One of them showed expression of desmin. Two of them occurred in the shoulder, and the third in the popliteal fossa. Two of them occurred in males and were classified as malignant, while the last one occurred in a woman and was benign. The index case OFMT3 showed, in addition to the mature shell of bone, focal areas of osteoid-like matrix deposition, surrounding individual tumor cells, reminiscent of an osteosarcoma (Fig. 1F).

EP400-PHF1 is the most common recurrent fusion in OFMT

PHF1 gene rearrangements were identified in 31/39 cases (80%). The most common fusion partner for *PHF1* was *EP400*, present in 17 (55%) cases (Figs. 1G, I–L, 4). Of these, 11 (69%) cases were positive for S100 protein (with two cases being only focal) and twelve (75%) showed reactivity for desmin. Ten cases showed typical peripheral ossification and were variably distributed within extremity, trunk and head and neck. Nine were classified as benign (53%), while the remaining were divided among atypical or malignant.

OFMT share *EPC1-PHF1* fusions with endometrial stromal sarcomas (ESS)

As *EPC1* and *JAZF1* have been described as additional gene partners involved in *PHF1* fusions in ESS, we hypothesized that similar gene fusions may be implicated in OFMT with *PHF1* gene rearrangements. Thus, 5 *PHF1*-rearranged OFMT cases lacking a fusion partner were tested by FISH for abnormalities in *JAZF1* and *EPC1*. Two of the 5 cases showed *EPC1* breakapart with an unbalanced telomeric deletion (Suplem Fig. 1, Table 1), while no *JAZF1* gene abnormalities were seen in any of the cases. Both *EPC1-PHF1* positive OFMT tumors were negative for S100 protein and one showed desmin reactivity.

PHF1-rearranged OFMT, lacking an identifiable fusion partner, is more often benign and S100 protein positive

Nine tumors were positive for *PHF1* break-apart by FISH, but lacked abnormalities in *EP400, MEAF6* and *EPC1*. No differences in anatomic location or morphology were noted

between the different *PHF1*-rearranged genetic subsets (Figs. 1H, O, P). All except one was benign and all 8 tumors tested were S100 protein positive. Six (75%) tumors showed desmin reactivity. Six tumors were located in the extremity, while three cases were in the head and neck.

Fifteen percent of OFMT are fusion-negative

There were 6 (15%) tumors that were negative for all FISH probes tested and no frozen tissue was available for further RNA sequencing (Table 2). Four of these lesions occurred in the trunk, two each in the back and axilla, while the remaining two lesions occurred in the hip and thigh area. All except one case was desmin positive, while three showed S100 protein positivity (focally in two cases). Two of them were benign, while the others were classified as malignant. There were no discernible differences in their morphologic appearance when compared to fusion-positive tumors; four of them showed the classic peripheral rim of lamellar bone. All tumors in this group were tested for *FUS* gene abnormalities to exclude the possibility of an unusual low grade fibromyxoid sarcoma, the closest diagnostic mimic to non-ossifying OFMT.

DISCUSSION

Ossifying fibromyxoid tumor (OFMT) is a rare and enigmatic soft tissue tumor, of uncertain histogenesis and until recently of unknown genetic abnormalities. It was initially defined by Enzinger as a subcutaneous tumor with a peripheral or septal shell of bone, lobulated growth, and small, bland cells arranged in cords and nests within a fibromyxoid stroma (Enzinger et al., 1989). Most OFMT are benign, however, reports have documented both cyto-architecturally and clinically atypical OFMT, including cases with histologic features of malignancy (generally including some combination of high cellularity, nuclear atypia, and elevated mitotic activity) and confirmed metastatic disease (Kilpatrick et al., 1995; Folpe and Weiss, 2003). The diagnosis of malignant OFMT remains challenging and somewhat controversial, since it has not always been defined or accepted as the cellular and mitotically active counterpart of conventional OFMT. As such, atypical variants were reported with minimal or no conventional OFMT component and/or lack of bone formation, and a lower rate of S100 protein expression (Folpe and Weiss, 2003). S100 protein was reported as being almost universally expressed in typical, benign OFMT (Miettinen et al., 2008), while malignant OFMT cases have a significantly lower rate of S100 reactivity (Folpe and Weiss, 2003). This immunophenotypic difference has been proposed by some as evidence that malignant lesions are fundamentally distinct from conventional OFMTs (Miettinen et al., 2008), while others suggested that loss of S100 protein may be related to malignant transformation (Folpe and Weiss, 2003). As Miettinen et al. pointed out, the lack of objective diagnostic criteria in some of the reported atypical/malignant cases questions their subclassification as OFMT (Miettinen et al., 2008). Thus the identification of an unifying genetic marker, such as a recurrent tumor-specific translocation, has long been needed for the apparently wide morphologic spectrum of OFMT, which could then help in defining the “outer limits” of this entity and resolve the nature of biologically malignant tumors with some OFMT-like features (Miettinen et al., 2008).

Gebre-Medhin et al (Gebre-Medhin et al., 2012) recently identified the presence of *PHF1* gene rearrangements on 6p21 in more than half of the OFMT lesions tested, with higher incidence in benign lesions (4/4) compared to malignant OFTs (1/6). In one of their tumors *PHF1* was fused to *EP400* on 12q24.3 (Gebre-Medhin et al., 2012). An additional OFMT case carrying a t(6;12)(p21;q24.3) resulting in a *EP400-PHF1* fusion has subsequently been reported in a 71 year-old female with a soft tissue mass in the palm (Endo et al., 2013). Furthermore, a very recent study screening a larger cohort of 41 OFMTs confirmed the incidence of *PHF1* gene rearrangements by FISH at nearly 50%, including roughly similar percentages of typical, atypical, and malignant tumors (Graham et al., 2013). The recurrent *PHF1* abnormalities identified in both typical and malignant OFMTs suggest a shared pathogenesis for these lesions and suggest the utility of FISH testing for *PHF1* gene rearrangements when diagnosing morphologically challenging cases. This is further supported by a gene expression profiling study, which showed extensive overlap between typical OFMT and the cases classified as malignant, in keeping with a single pathologic entity (Graham et al., 2011).

The PHF1 protein interacts with the polycomb-repressive complex 2 (PRC2), which, in turn, regulates the expression of a variety of developmental genes. *PHF1* encodes the PHD finger protein 1 (PHF1), which is involved in chromatin structure regulation, forming Polycomb repressive complex 2 (PRC2) with EZH1, EZH2, SUZ12, regulating histone H3 at lysine 27 (H3K27) methylation.

RNA sequencing, followed by FusionSeq data analysis, in one of the index cases (OFMT1) showed the presence of a t(X;22)(p11;q13) translocation resulting in a *ZC3H7B-BCOR* fusion. A similar translocation has recently been identified in two cases of endometrial stromal sarcoma (Panagopoulos et al., 2013). Interestingly of the three patients with available karyotypes in the study of Gebre-Medhin et al, two cases that were positive for *PHF1* gene rearrangements but negative for *EP400* by FISH, showed an Xp11 locus abnormality, either involving a standard translocation with 6p, or in a three-way exchange with chromosomes 6 and 7 (Gebre-Medhin et al., 2012). Based on our findings, these cases with Xp11 locus rearrangements would suggest *BCOR* gene fusions. *BCOR* gene rearrangements have recently been described in a subset of small blue round cell tumors, as the 5′ fusion partner to *CCNB3* (encoding the testis-specific cyclin B3, which induces oncogenic activation of the CCNB3 protein (Pierron et al., 2012). In contrast, in the OFMT setting, *BCOR*, encoding for BCL6 co-repressor, is the 3′ partner in the fusion with *ZC3H7B*, resulting in *BCOR* mRNA expression, suggesting a different mechanism of oncogenesis. Additionally a *BCOR-RARA* fusion has been reported in a variant of acute promyelocytic leukemia, resulting in a dominant-negative manner on RARA transcriptional activation (Yamamoto et al., 2010).

PHF1 rearrangements have previously been associated with endometrial stromal sarcoma (ESS), in that context being fused with either *JAZF1* or *EPC1* (Micci et al., 2006). The *JAZF1-PHF1* and *EPC1-PHF1* fusions account for a minority (9%) of ESS cases and have not been detected in benign endometrial stromal nodules (Chiang et al., 2011). The *PHF1*-chromosomal rearrangements are highly complex in both tumor types (Micci et al., 2006; Gebre-Medhin et al., 2012), and, due to the transcriptional orientation of the genes, neither

JAZF1-PHF1 nor *EPC1-PHF1* fusions can arise through a simple translocation (Micci et al., 2006). As seen in our OFMT3, *PHF1*-rearranged ESS showed a similar breakpoint within intron 1, thus the entire PHF1 coding region is translated in the chimeric protein, including its tudor, PHD zinc finger and MTF2 domains (Panagopoulos et al., 2012). Furthermore, similar with ESS pathogenesis, it appears that translocation genes involved in acetylation (*MEAF6, EPC1*) and methylation (*PHF1*) have a role in the neoplastic development of OFMT. *EPC1* encodes a member of the polycomb group (PcG) family, which is a component of the NuA4 histone acetyltransferase complex and can act as both a transcriptional activator and repressor. Potential mistargeted acetylation or methylation most likely results in loosening of the heterochromatin and induction of aberrant gene expression. In light of our present findings, the recent case report of a cardiac ossifying sarcoma of non-endometrial stromal origin most likely represents a malignant OFMT, showing the *JAZF1-PHF1* (Schoolmeester et al., 2013).

Furthermore, *MEAF6-PHF1*fusion has been described in one ESS from a 43 year-old female with classic morphology (Panagopoulos et al., 2012). MEAF6 is ubiquitously expressed and encodes a protein which is part of the histone acetyltransferase multisubunit complexes of the MYST family. The MYST histone acetyltransferases are highly conserved in eukaryotes and carry out a significant proportion of all nuclear acetylation, playing a critical role in gene-specific transcriptional regulation, DNA damage and repair (Cai et al., 2003; Avvakumov and Cote, 2007).

The presence of identical chromosomal translocations in ESS and OFMT, two pathologic entities with no morphologic or immunophenotypic overlap, is quite intriguing, although shared abnormalities have been described in a variety of other seemingly unrelated tumors, including *EWSR1-CREB1* in angiomatoid fibrous histiocytoma and clear cell sarcoma (Antonescu et al., 2006; Antonescu et al., 2007), *ETV6-NTRK3* in infantile fibrosarcoma, leukemia and secretory breast carcinoma (Knezevich et al., 1998; Tognon et al., 2002), and *ALK*-gene rearrangements in inflammatory myofibroblastic tumor, lung carcinoma and lymphoma (Morris et al., 1994; Lawrence, 2000; Soda et al., 2007).

In summary, our study identified three novel fusions *ZC3H7B-BCOR, MEAF6-PHF1* and *EPC1-PHF1* in OFMTs. With these additional gene fusions, the majority (85%) of OFMTs with classic morphologic appearances demonstrated recurrent gene rearrangements, regardless of the degree of malignancy, presence of ossification or immunoprofile, which can therefore be used as molecular markers in challenging cases. The most common abnormality is *PHF1* gene rearrangement (80%), being present in benign, atypical and malignant lesions, with fusion to *EP400* in 44% of cases. *ZC3H7B-BCOR, MEAF6-PHF1* and *EPC1-PHF1* fusions occurred predominantly in S100 protein-negative and malignant OFMT. Similar gene fusions have been reported in endometrial stromal sarcoma, a tumor seemingly unrelated to OFMT.

Supplementary Material

Refer to Web version on PubMed Central for supplementary material.

Acknowledgments

We thank Agnes Viale and the Genomic Core Lab for the excellent expertise with RNA sequencing and Milagros Soto for editorial assistance.

Supported in part by: P01CA47179 (CRA, SS), P50 CA 140146-01 (CRA, SS).

References

Antonescu CR, Dal Cin P, Nafa K, Teot LA, Surti U, Fletcher CD, Ladanyi M. EWSR1-CREB1 is the predominant gene fusion in angiomatoid fibrous histiocytoma. Genes Chromosomes Cancer. 2007; 46:1051–1060. [PubMed: 17724745]

Antonescu CR, Nafa K, Segal NH, Dal Cin P, Ladanyi M. EWS-CREB1: a recurrent variant fusion in clear cell sarcoma--association with gastrointestinal location and absence of melanocytic differentiation. Clin Cancer Res. 2006; 12:5356–5362. [PubMed: 17000668]

Antonescu CR, Zhang L, Chang NE, Pawel BR, Travis W, Katabi N, Edelman M, Rosenberg AE, Nielsen GP, Dal Cin P, Fletcher CD. EWSR1-POU5F1 fusion in soft tissue myoepithelial tumors. A molecular analysis of sixty-six cases, including soft tissue, bone, and visceral lesions, showing common involvement of the EWSR1 gene. Genes Chromosomes Cancer. 2010; 49:1114–1124. [PubMed: 20815032]

Avvakumov N, Cote J. The MYST family of histone acetyltransferases and their intimate links to cancer. Oncogene. 2007; 26:5395–5407. [PubMed: 17694081]

Cai Y, Jin J, Tomomori-Sato C, Sato S, Sorokina I, Parmely TJ, Conaway RC, Conaway JW. Identification of new subunits of the multiprotein mammalian TRRAP/TIP60-containing histone acetyltransferase complex. J Biol Chem. 2003; 278:42733–42736. [PubMed: 12963728]

Chiang S, Ali R, Melnyk N, McAlpine JN, Huntsman DG, Gilks CB, Lee CH, Oliva E. Frequency of known gene rearrangements in endometrial stromal tumors. Am J Surg Pathol. 2011; 35:1364–1372. [PubMed: 21836477]

Dobin A, Davis CA, Schlesinger F, Drenkow J, Zaleski C, Jha S, Batut P, Chaisson M, Gingeras TR. STAR: ultrafast universal RNA-seq aligner. Bioinformatics. 2013; 29:15–21. [PubMed: 23104886]

Endo M, Kohashi K, Yamamoto H, Ishii T, Yoshida T, Matsunobu T, Iwamoto Y, Oda Y. Ossifying fibromyxoid tumor presenting EP400-PHF1 fusion gene. Hum Pathol. 2013; 44:2603–2608. [PubMed: 23806526]

Enzinger FM, Weiss SW, Liang CY. Ossifying fibromyxoid tumor of soft parts. A clinicopathological analysis of 59 cases. Am J Surg Pathol. 1989; 13:817–827. [PubMed: 2476942]

Folpe AL, Weiss SW. Ossifying fibromyxoid tumor of soft parts: a clinicopathologic study of 70 cases with emphasis on atypical and malignant variants. Am J Surg Pathol. 2003; 27:421–431. [PubMed: 12657926]

Gebre-Medhin S, Nord KH, Moller E, Mandahl N, Magnusson L, Nilsson J, Jo VY, Vult von Steyern F, Brosjo O, Larsson O, Domanski HA, Sciot R, Debiec-Rychter M, Fletcher CD, Mertens F. Recurrent rearrangement of the PHF1 gene in ossifying fibromyxoid tumors. Am J Pathol. 2012; 181:1069–1077. [PubMed: 22796436]

Graham RP, Dry S, Li X, Binder S, Bahrami A, Raimondi SC, Dogan A, Chakraborty S, Souchek JJ, Folpe AL. Ossifying fibromyxoid tumor of soft parts: a clinicopathologic, proteomic, and genomic study. Am J Surg Pathol. 2011; 35:1615–1625. [PubMed: 21997683]

Graham RP, Weiss SW, Sukov WR, Goldblum JR, Billings SD, Dotlic S, Folpe AL. PHF1 Rearrangements in Ossifying Fibromyxoid Tumors of Soft Parts: A Fluorescence In Situ Hybridization Study of 41 Cases With Emphasis on the Malignant Variant. Am J Surg Pathol. 2013; 37:1751–1755. [PubMed: 23887158]

Habegger L, Sboner A, Gianoulis TA, Rozowsky J, Agarwal A, Snyder M, Gerstein M. RSEQtools: a modular framework to analyze RNA-Seq data using compact, anonymized data summaries. Bioinformatics. 2011; 27:281–283. [PubMed: 21134889]

Kilpatrick SE, Ward WG, Mozes M, Miettinen M, Fukunaga M, Fletcher CD. Atypical and malignant variants of ossifying fibromyxoid tumor. Clinicopathologic analysis of six cases. Am J Surg Pathol. 1995; 19:1039–1046. [PubMed: 7661277]

Knezevich SR, McFadden DE, Tao W, Lim JF, Sorensen PH. A novel ETV6-NTRK3 gene fusion in congenital fibrosarcoma. Nat Genet. 1998; 18:184–187. [PubMed: 9462753]

Lawrence B, Perez-Atayde A, Hibbard MK, Rubin BP, Dal Cin P, Pinkus JL, Pinkus GS, Xiao S, Yi ES, Fletcher CD, Fletcher JA. TPM3-ALK and TPM4-ALK oncogenes in inflammatory myofibroblastic tumors. Am J Pathol. 2000; 157:377–384. [PubMed: 10934142]

Micci F, Panagopoulos I, Bjerkehagen B, Heim S. Consistent rearrangement of chromosomal band 6p21 with generation of fusion genes JAZF1/PHF1 and EPC1/PHF1 in endometrial stromal sarcoma. Cancer Res. 2006; 66:107–112. [PubMed: 16397222]

Miettinen M, Finnell V, Fetsch JF. Ossifying fibromyxoid tumor of soft parts--a clinicopathologic and immunohistochemical study of 104 cases with long-term follow-up and a critical review of the literature. Am J Surg Pathol. 2008; 32:996–1005. [PubMed: 18469710]

Morris SW, Kirstein MN, Valentine MB, Dittmer KG, Shapiro DN, Saltman DL, Look AT. Fusion of a kinase gene, ALK, to a nucleolar protein gene, NPM, in non-Hodgkin's lymphoma. Science. 1994; 263:1281–1284. [PubMed: 8122112]

Mosquera JM, Sboner A, Zhang L, Kitabayashi N, Chen CL, Sung YS, Wexler LH, Laquaglia MP, Edelman M, Sreekantaiah C, Rubin MA, Antonescu CR. Recurrent NCOA2 gene rearrangements in congenital/infantile spindle cell rhabdomyosarcoma. Genes Chromosomes Cancer. 2013; 52:538–550. [PubMed: 23463663]

Panagopoulos I, Micci F, Thorsen J, Gorunova L, Eibak AM, Bjerkehagen B, Davidson B, Heim S. Novel fusion of MYST/Esa1-associated factor 6 and PHF1 in endometrial stromal sarcoma. PLoS One. 2012; 7:e39354. [PubMed: 22761769]

Panagopoulos I, Thorsen J, Gorunova L, Haugom L, Bjerkehagen B, Davidson B, Heim S, Micci F. Fusion of the ZC3H7B and BCOR genes in endometrial stromal sarcomas carrying an X;22-translocation. Genes Chromosomes Cancer. 2013; 52:610–618. [PubMed: 23580382]

Pierron G, Tirode F, Lucchesi C, Reynaud S, Ballet S, Cohen-Gogo S, Perrin V, Coindre JM, Delattre O. A new subtype of bone sarcoma defined by BCOR-CCNB3 gene fusion. Nat Genet. 2012; 44:461–466. [PubMed: 22387997]

Quail MA, Kozarewa I, Smith F, Scally A, Stephens PJ, Durbin R, Swerdlow H, Turner DJ. A large genome center's improvements to the Illumina sequencing system. Nat Methods. 2008; 5:1005–1010. [PubMed: 19034268]

Sboner A, Habegger L, Pflueger D, Terry S, Chen DZ, Rozowsky JS, Tewari AK, Kitabayashi N, Moss BJ, Chee MS, Demichelis F, Rubin MA, Gerstein MB. FusionSeq: a modular framework for finding gene fusions by analyzing paired-end RNA-sequencing data. Genome Biol. 2010; 11:R104. [PubMed: 20964841]

Schoolmeester JK, Sukov WR, Maleszewski JJ, Bedroske PP, Folpe AL, Hodge JC. JAZF1 rearrangement in a mesenchymal tumor of nonendometrial stromal origin: report of an unusual ossifying sarcoma of the heart demonstrating JAZF1/PHF1 fusion. Am J Surg Pathol. 2013; 37:938–942. [PubMed: 23629446]

Soda M, Choi YL, Enomoto M, Takada S, Yamashita Y, Ishikawa S, Fujiwara S, Watanabe H, Kurashina K, Hatanaka H, Bando M, Ohno S, Ishikawa Y, Aburatani H, Niki T, Sohara Y, Sugiyama Y, Mano H. Identification of the transforming EML4-ALK fusion gene in non-small-cell lung cancer. Nature. 2007; 448:561–566. [PubMed: 17625570]

Tanas MR, Sboner A, Oliveira AM, Erickson-Johnson MR, Hespelt J, Hanwright PJ, Flanagan J, Luo Y, Fenwick K, Natrajan R, Mitsopoulos C, Zvelebil M, Hoch BL, Weiss SW, Debiec-Rychter M, Sciot R, West RB, Lazar AJ, Ashworth A, Reis-Filho JS, Lord CJ, Gerstein MB, Rubin MA, Rubin BP. Identification of a disease-defining gene fusion in epithelioid hemangioendothelioma. Sci Transl Med. 2011; 3:98ra82.

Tognon C, Knezevich SR, Huntsman D, Roskelley CD, Melnyk N, Mathers JA, Becker L, Carneiro F, MacPherson N, Horsman D, Poremba C, Sorensen PH. Expression of the ETV6-NTRK3 gene fusion as a primary event in human secretory breast carcinoma. Cancer Cell. 2002; 2:367–376. [PubMed: 12450792]

Yamamoto Y, Tsuzuki S, Tsuzuki M, Handa K, Inaguma Y, Emi N. BCOR as a novel fusion partner of retinoic acid receptor alpha in a t(X;17)(p11;q12) variant of acute promyelocytic leukemia. Blood. 2010; 116:4274–4283. [PubMed: 20807888]

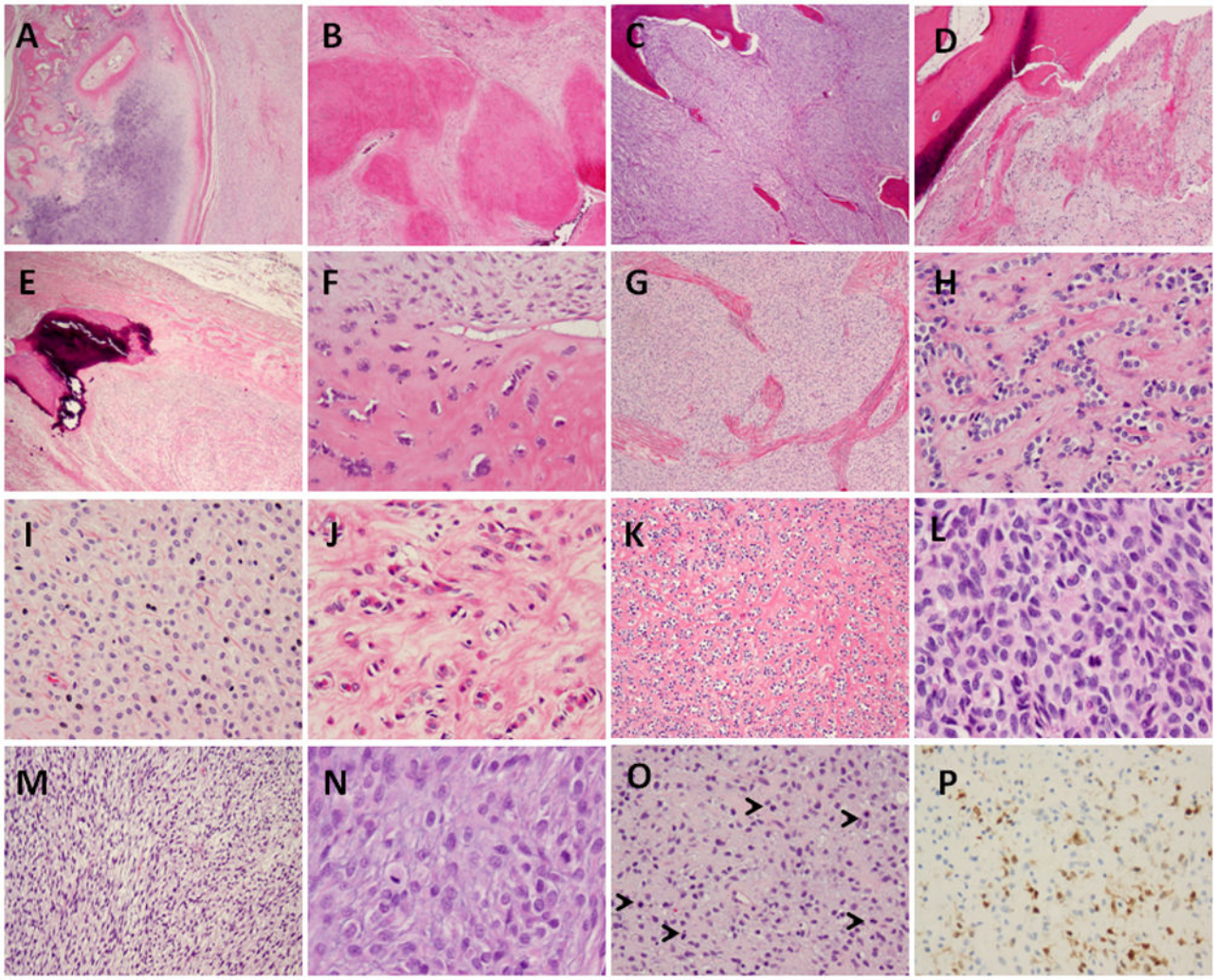

Figure 1.

Morphologic spectrum of OFMT harboring different fusion transcript types. Low power reveals a thick peripheral rim of lamellar bone accompanied by an incomplete cartilaginous cap (A), other areas showed densely hyalinized nodules, lacking mineralization (B), while central areas showed the cellular component admixed with lamellar bone (C) (A–C, OFMT1, *ZC3H7B-BCOR* fusion); (D) Peripheral ossification in OFMT3 showing *MEAF6-PHF1;* (E) benign OFMT showing partly ossified partly hyalinized pseudocapsule (OFMT7, *EP400-PHF1* fusion); (F) a subset of malignant OFMT showed lesional cells embedded within osteoid matrix, reminiscent of osteosarcoma (OFMT3, *MEAF6-PHF1*); or (G) thick fibrous bands separating the tumor into broad compartments (OFMT14, *EP400-PHF1*); (H) Benign OFMT with classic cord-like arrangement separated by a dense collagenous stroma (OFMT26, *PHF1* rearranged); (I) epithelioid phenotype with more abundant eosinophilic cytoplasm (OFMT15, *EP400-PHF1*); or (J) a distinctive rhabdoid appearance (OFMT7, *EP400-PHF1*); (K) malignant OFMT showing a biphasic appearance composed of a benign hypocellular component associated with a conspicuous fibrous stroma, in abrupt transition to a (L) malignant cellular component with high mitotic activity (OFMT21, *EP400-PHF1*);

(M) rare cases of malignant OFMT showed a more spindled/fusiform appearance, arranged in short intersecting fascicles (OFMT20, *EP400-PHF1*); (N) Most malignant OFMT showed increased cellularity and mitotic activity (OFMT1, *ZC3H7B-BCOR*); (O) with a loose extracellular stroma and focally very high mitotic activity (5 mitoses, highlighted with arrows) (OFMT33, *PHF1* rearranged). (P) The pattern of S100 protein reactivity in malignant OFMT was typically focal (OFMT33, *PHF1* rearranged).

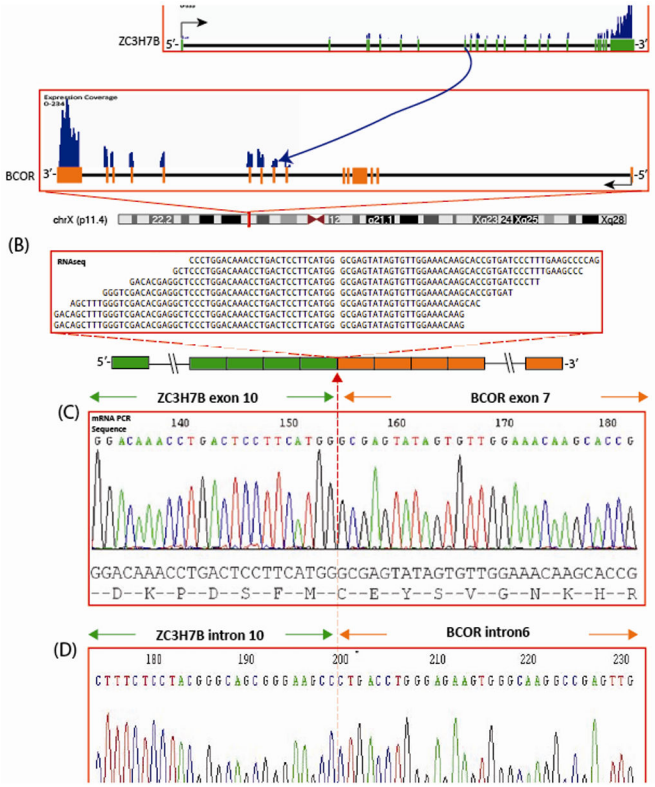

Figure 2.

ZC3H7B-BCOR gene fusion in malignant ossifying fibromyxoid tumor (OFMT1). (A) Schematic representation of the *ZC3H7B-BCOR* fusion indicating the loci that are joint together; *ZC3H7B* exon 10 being fused to *BCOR* exon 7; (B) RNA reads covering the fusion junction were isolated independent to FusionSeq analysis work flow, supporting the *ZC3H7B-BCOR* fusion candidate; (C) Experimental validation of the fusion by RT-PCR shows the junction sequence between exon 10 of *ZC3H7B* and exon 7 of *BCOR*; (D) Long range DNA PCR showing the fusion of intron 10 of *ZC3H7B* to the intron 6 of *BCOR*.

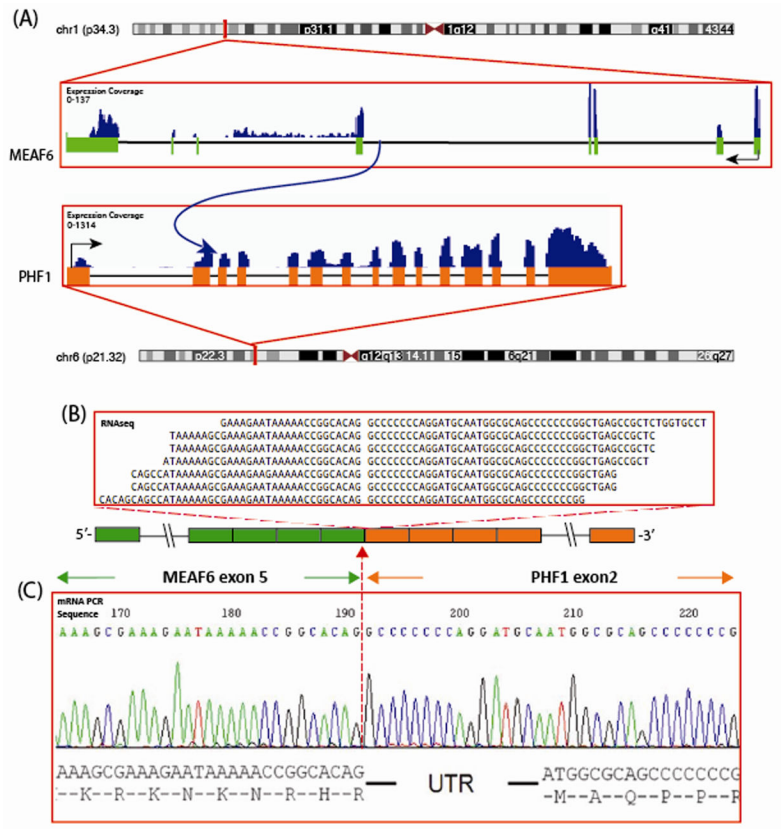

Figure 3.

MEAF6-PHF1 gene fusion in malignant ossifying fibromyxoid tumor (OFMT3). (A) Schematic representation of the *MEAF6-PHF1* fusion indicating the loci that are joint together; *MEAF6* exon 5 being fused to *PHF1* exon 2; (B) RNA reads covering the fusion junction were isolated independent to FusionSeq analysis work flow, supporting this fusion candidate; (C) Experimental validation of the fusion by RT-PCR shows the junction sequence between exon 5 of *MEAF6* to exon 2 of *PHF1*.

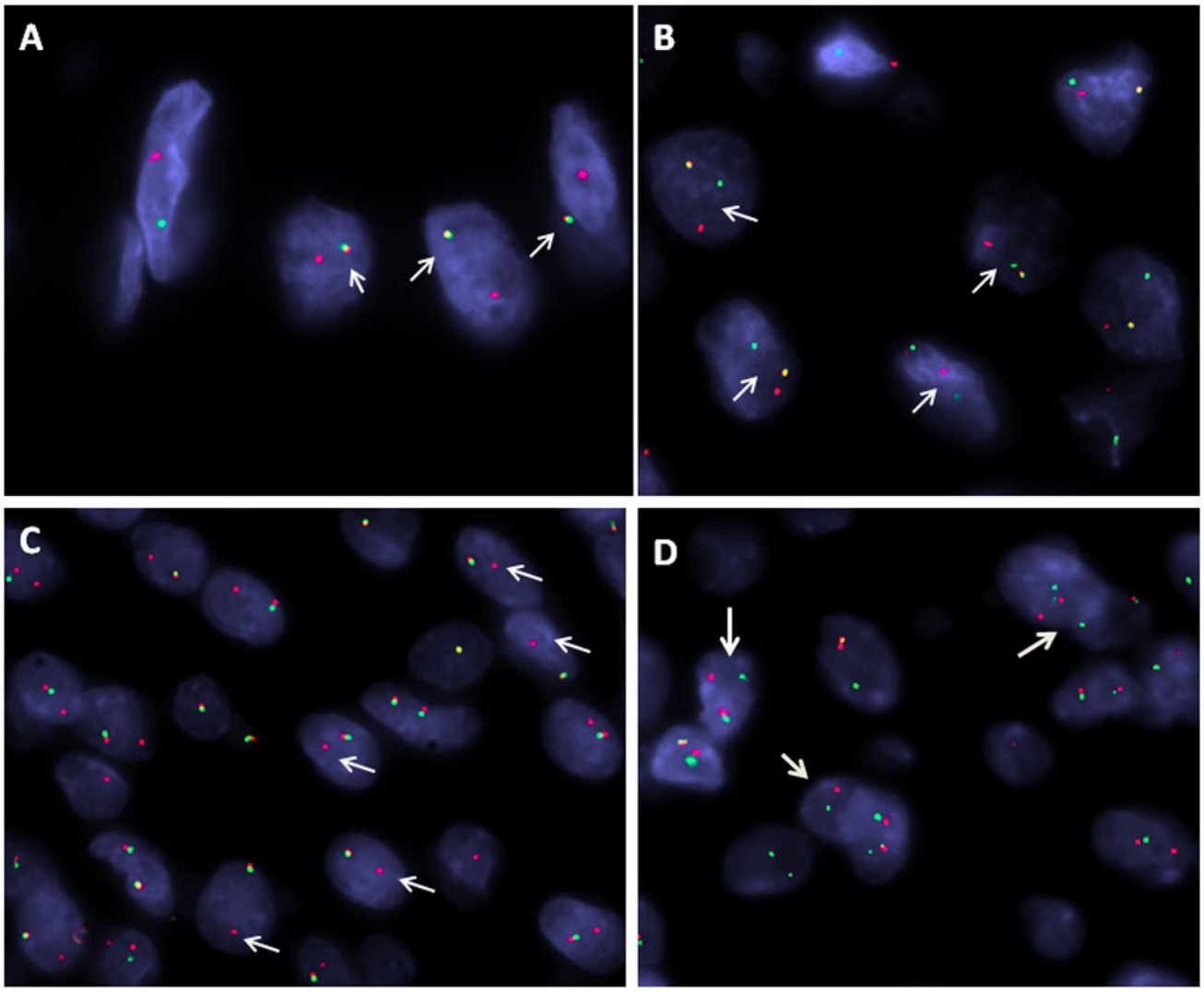

Figure 4.

FISH validation of OFMT-related gene rearrangements. (A) Fusion assay with *BCOR* (green, telomeric) and *ZC3H7B* (red, centromeric) showing one yellow fused signal (OFMT1, male patient, only one *BCOR* allele on Xp11); (B) Break-apart assay showing a split *MEAF6* signal (OFMT4; red centromeric, green telomeric); (C) Unbalanced *EP400* gene rearrangement, showing break-apart signal with deletion of telomeric (green) part (OFMT14; red, centromeric); (D) *PHF1* break apart signal (OFMT14; red centromeric, green, telomeric).

Table 1

Clinical and Pathologic Findings of OFMTs showing gene rearrangements

OFMT	Age/ Sex	Location	Histology	S100	Desmin	Fusion/Re- arrangement
1*	55/M	groin/thigh	Malignant, ossifying	Neg	Neg	ZC3H7B-BCOR
2	76/M	Thigh	Malignant, ossifying	Neg	Neg	BCOR
3*	73/M	popliteal	Malignant, ossifying	Neg	Neg	MEAF6-PHF1
4	38/M	Shoulder	Malignant, ossifying	Neg	Neg	MEAF6-PHF1
5	66/F	Shoulder	Benign, ossifying	Neg	Pos	MEAF6-PHF1
6	56/F	Shoulder	Malignant, ossifying	Neg	Fpos	EP400-PHF1
7	24/F	Buttock	Benign, ossifying	Fpos	Fpos	EP400-PHF1
8	38/F	Thigh	Benign, ossifying	Pos	Neg	EP400-PHF1
9	48/M	Axilla	Benign, ossifying	Neg	Neg	EP400-PHF1
10	21/F	Thigh	Benign, non-ossifying	Pos	Neg	EP400-PHF1
11	73/M	Foot	Benign, non-ossifying	Pos	Neg	EP400-PHF1
12	46/F	skin, breast	Benign, non-ossifying	Pos	Pos	EP400-PHF1
13	23/F	Thigh	Benign, non-ossifying	Pos	Pos	EP400-PHF1
14	48/F	Neck	Benign, non-ossifying	Pos	Pos	EP400-PHF1
15	43/F	Buttock	Benign, non-ossifying	Pos	Pos	EP400-PHF1
16	65/F	Leg	Atypical, ossifying	N/A	N/A	EP400-PHF1
17	70/M	Neck	Atypical, ossifying	Pos	Pos	EP400-PHF1
18	69/F	supraclavicular	Atypical, ossifying	Pos	Pos	EP400-PHF1
19	59/F	Shoulder	Malignant, ossifying	Fpos	Pos	EP400-PHF1
20	69/F	chest wall	Malignant, ossifying	Neg	Pos	EP400-PHF1
21	41/F	Breast	Malignant, ossifying	Neg	Pos	EP400-PHF1
22	59/F	Paraspinal	Malignant, non-ossifying	Neg	Pos	EP400-PHF1
23	69/M	Thigh	Benign, non-ossifying	Neg	Pos	EPC1-PHF1
24	41/M	Forearm	Malignant, ossifying	Neg	Neg	EPC1-PHF1
25	49/F	supraclavicular	Benign, ossifying	N/A	N/A	PHF1
26	60/M	Finger	Benign, ossifying	Pos	Pos	PHF1

OFMT	Age/ Sex	Location	Histology	S100	Desmin	Fusion/Re- arrangement
27	71/M	Hand	Benign, ossifying	Pos	Neg	PHF1
28	65/F	Tongue	Benign, ossifying	Pos	Pos	PHF1
29	32/M	Foot	Benign, non-ossifying	Pos	Fpos	PHF1
30	70/M	Cheek	Benign, non-ossifying	Pos	Pos	PHF1
31	55/F	Foot	Benign, non-ossifying	Pos	Pos	PHF1
32	72/F	Foot	Benign, non-ossifying	Pos	Pos	PHF1
33	59/M	Leg	Malignant, non-ossifying	Fpos	Neg	PHF1

* index cases tested for RNAseq; F, female; M, male; Pos, positive; Neg, negative; Fpos, focally positive; N/A, not available.

Table 2

Clinical and Pathologic Findings in Translocation-Negative OFMT (n=6)

OFMT	Age/ Sex	Location	Histology	S100	Desmin
34	53/M	back	Benign, non-ossifying	Pos	Pos
35	34/F	axilla	Benign, non-ossifying	Neg	Pos
36	71/F	hip	Malignant, ossifying	Fpos	Pos
37	24/M	back	Malignant, ossifying	Neg	Pos
38	51/M	axilla	Malignant, ossifying	Fpos	Neg
39	70/F	thigh	Malignant, ossifying	Neg	Pos

F, female; M, male; Pos, positive; Neg, negative; Fpos, focally positive.